Direct evaluation of the hopping rate in Langmuir multilayer assemblies

Michio Sugi, Tsunekatsu Fukui, and Sigeru Iizima
Electrotechnical Laboratory, Mukodai, Tanashi, Tokyo, Japan
(Received 12 December 1977)

Conductivity dispersion has been observed in the heterogeneous assemblies of Cd-palmitate and Cd-arachidate monolayers prepared using the Langmuir-Blodgett technique. The transition rate of hopping carriers in Cd-palmitate monolayers has been directly evaluated from the dispersion frequency by applying the theory presented in the previous paper. The rate values agree with those calculated for Cd-palmitate employing the corrected layer thickness allowing for a finite thickness of interface layers. Comparison with the theoretical predictions has confirmed the validity of the single-rate scheme with nearest-neighbor approximation as an appropriate model to describe the actual system. The results indicate, however, the inadequacy of the evaluation of effective carrier concentration based on a two-dimensional degenerate electron system adopted in the earlier works, whereas the values of other parameters agree in order of magnitude with those estimated before.

I. INTRODUCTION

In a previous paper[1] we have developed the theory of frequency-dependent conductivity in assemblies of insulating monomolecular layers (monolayers) as a hopping system. The model considered in this study refers to electronic conduction based on the hopping mechanism, allowing for the multilayer structure as a planar distribution of localized states at each interface between insulating layers.[2] Each constituent layer is then characterized by a single rate for carriers at a certain energy level to traverse the layer. The rate is determined by the layer thickness l, the wave-function damping constant $\alpha(E)$, and the interface state density $N'(E)$, and expressed as

$$\lambda(E,l)=\lambda_0[2\alpha(E)]^{3/2} \times \exp\left[-2\alpha l-\left(\frac{4\alpha}{\pi N'(E)lkT}\right)^{1/2}\right], \quad (1)$$

which has appropriately explained the dc conductivity of homogeneous assemblies of monolayers of Cd salts of fatty acids, $CH_3-(CH_2)_{n-2}-COOH$ with $n=16$, 18, or 20.[3-5]

The motion of carriers has been treated as a continuous-time random walk on a one-dimensional array of interfaces, each connected to the neighbors with uniquely defined rates, by applying the extended Montroll-Weiss formalism.[6] For heterogeneous assemblies consisting of different layers, a frequency dispersion of the conductivity has been predicted as characteristic of each superstructure in the layer sequence, while the homogeneous assemblies have been found to show a frequency-independent conductivity. The dispersion frequency, in contrast to the Maxwell-Wagner-type interface polarization, has been immediately related to the one-layer transition rate.

If the unit cell of a heterogeneous assembly consists of M monolayers with the larger rate λ_1 and one monolayer with the smaller rate $\lambda_2(\lambda_1 >> \lambda_2)$ for carriers near the Fermi level, the dark conductivity is approximated as

$$\sigma(\omega)=(M+1)\sigma_2 + \frac{M\sigma_1[\omega K(M)/\lambda_1]^2}{(M+1)\{1+[\omega K(M)/\lambda_1]^2\}}, \quad (2)$$

where ω is the angular frequency and $K(M)/\lambda_1$ is the largest finite relaxation time in the unit array of $M+1$ interfaces. In Eq. (2), σ_1 and σ_2 are the frequency-independent (dc) conductivities of the corresponding homogeneous assemblies of layers 1 and 2, respectively, each given by

$$\sigma=(e^2/kT)n'l^2\lambda, \quad (3)$$

where λ, l, and n' are the rate, the layer thickness, and the effective carrier concentration.

The dielectric constant $\epsilon(\omega)$ is given as

$$\epsilon(\omega)=\epsilon(\infty)+\frac{M\sigma_1[K(M)/\lambda_1]}{(M+1)\{1+[\omega K(M)/\lambda_1]^2\}} \quad (4)$$

by means of the Kramers-Kronig relation, where $\epsilon(\infty)$ refers to the value for $\omega >> \lambda_1/K(M)$.

In the earlier works,[3-5] the layer thickness was simply represented by half of the length d of a bilayer unit cell of the pure homogeneous assembly. The effective carrier concentration n' for the dark-conductivity case, on the other hand, was evaluated by assuming a strongly degenerate electron system with slowly varying interface state density $N'(E)$,

$$n'=2kTN'(E_F)/l \quad (5)$$

By these approximations, the dc conductivities in the dark case were qualitatively fairly well explained.

Our recent study of multilayer structure[7] has, however, aroused a question as for whether $l = \frac{1}{2}d$ is justified as a realistic evaluation for the thickness of insulating layers. The bilayer unit cell is, according to our results, associated with an electron-deficient layer several angstroms thick. This indicates that a correction of l is required, assuming a finite thickness for each interface, which is reflected in the very existence of such an electron-deficient layer. The transition rate λ has been estimated by taking $l = nd/(2n+5)$ as the "effective thickness," which should correspond to the distance between both end groups (CH_3- and -COO^-) of a fatty-acid residue with n carbon atoms in the straightened conformation forming the monolayers. They were $\lambda/2\pi = 10^{-1}$–10^{-2} Hz, 10^{-2}–10^{-3} Hz, and around 10^{-4} Hz for palmitate ($n=16$), stearate ($n=18$), and arachidate ($n=20$), respectively, as given in the previous paper.[1]

The above quoted values are, however, several decades larger than those obtained for $l = \frac{1}{2}d$. This means that the physically reasonable correction of l is rather incompatible with the evaluation of n' [Eq. (5)] adopted in the earlier works,[3–5] since the $N'(E_F)$ value, if correspondingly corrected, will no more give the reasonable temperature dependence in Eq. (1).

The experimental crucial check of the framework of the hopping theory so far developed was performed by examining the validity of the dispersion-phenomenon predictions and then the behavior of λ and n' independently, employing heterogeneous assemblies of Cd-palmitate and Cd-arachidate monolayers. We have observed the conductivity dispersion and obtained λ in agreement with the value estimated for the corrected layer thickness of palmitate monolayers. The results are presented together with a discussion.

In the following sections, we will use the abbreviations, C_n and $[C_n]$, for a fatty acid with n carbon atoms, each referring to the salt, $Cd[CH_3\text{-}(CH_2)_{n-2}\text{-}COO]_2$, or the radical, $[CH_3\text{-}(CH_2)_{n-2}\text{-}COO]^-$.

II. EXPERIMENTAL

A. Sample preparation

The metal-film-metal junctions were fabricated using the molecular assembly technique developed by Kuhn *et al.*[8] on the basis of the Langmuir-Blodgett technique.[9]

The substrates, each $\frac{1}{4}$ of an ordinary slide glass (13 mm × 38 mm, and 1.2-mm thick), were, after a preliminary ultrasonic cleaning, put in a saturated solution of KOH in ethanol for 4 to 5 hours, rinsed in an ultrasonic bath with bidistilled water, and then dried in a hot ambient (80–85 °C). The base and top electrodes were of Al (99.9999%) vacuum-evaporated films formed on the substrate under a pressure $<10^{-5}$ Torr before and after the deposition of monolayers, respectively.

The sample geometry is illustrated in Fig. 1 together with the junction structure. Three junctions of contact area approximately 0.2 cm^2 were formed on each substrate.

All multilayer films used in the experiment were Y-type films,[9] which are formed by alternate stacking of hydrophilic-to-hydrophilic and hydrophobic-to-hydrophobic contacts of monolayer surfaces. The heterogeneous films used involved one Cd-arachidate and either six or eight Cd-palmitate layers. The homogeneous films to be referred to were seven-layer assembly films. The Cd-salt monolayer was prepared by spreading a 5×10^{-3} M solution of the fatty acid [either arachidic acid (synthetic) from Eastman Kodak Co., Rochester, N. Y., palmitic acid (for gaschromatography) from Fluka AG, Buchs, Switzerland, or a mixture of both] in chloroform (spectro-grade, Tokyo Kasei Co., Tokyo, Japan) on a subphase of $4\times10^{-4}M$ $CdCl_2$ in bidistilled water. The pH value of the subphase was controlled by adding a small amount of either HCl or $KHCO_3$ to ensure conditions appropriate for both palmitate (C_{16}) and arachidate (C_{20}) under a surface pressure of approximately 25 dyn/cm. It was found that the pH value and the subphase temperature are linearly correlated with each other. The ranges chosen for the preparation extended from a pH of 6.2–6.3 for 16 °C up to a pH of 6.5–6.6 for 23 °C.

By means of the electron-diffraction technique, the two-dimensional concentrations of fatty-acid residues of a monolayer on an Al-coated substrate were evaluated as $(4.2+0.4)\times10^{14}$ cm^{-2} and $(4.3+0.4)\times10^{14}$ cm^{-2} for palmitate and arachidate, respectively.[10]

B. Electric measurement

The circuits for electric measurements are shown in Figs. 2(a) and 2(b). In (a), the real and imaginary

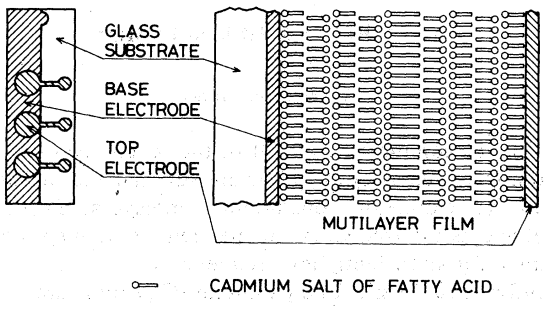

FIG. 1. Schematic representation of the sample geometry and assembly structure. The cross section of the nine-layer heterogeneous-assembly film is shown at right.

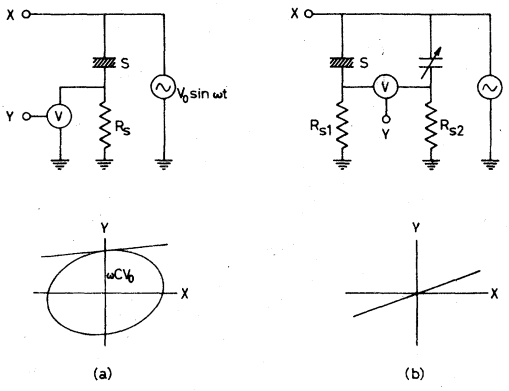

FIG. 2. Measuring circuits and the recorder traces. In (a), G and C are given as the slope of tangent and the intersection at $X=0$, while in (b) C is canceled with a reference capacitor. The voltmeters used are Keithley 610 C and 604 for (a) and (b), respectively.

parts of the sample admittance $Y=G+i\omega C$ were obtained graphically from the Lissajous's figure as the slope of the tangent and the intersection with the current axis, while in (b), the imaginary part was cancelled with a reference admittance $Y_r=G_r+i\omega C_r$ with $C_r=C$ and $G_r<10^{-12}$ mho (selected low-loss mica capacitors kept at liquid-nitrogen temperature). The series resistors R_s were so chosen that $\omega^2 R_s^2 C^2/G<0.1$ for (a) and <1 for (b) to eliminate the Maxwell-Wagner component due to R_s or the difference $|R_{s1}-R_{s2}|$. We preferred (a) to (b) as far as possible because of the relative simplicity of the measurement of (a).

The peak value of the ac applied voltage was smaller than 150 mV. The limit of measurement was up to 3×10^{-1} Hz in frequency and $G/\omega C(=\tan\delta)\gtrsim10^{-2}$ in loss factor, respectively.

Each sample was sealed in a cryostat with silica gel after storage for more than five days for measurement at room temperature.[5] The measurement at liquid-nitrogen temperature was carried out by immersing the sample directly into the liquid.[3]

III. RESULTS AND DISCUSSION

A. dc conductance

The dc conductances $G(0)$ of the seven-layer homogeneous-assembly films are summarized in Table I to characterize the constituent monolayers; $G(0)$ is defined as the frequency-independent component obtained for suffiiciently low frequencies ($\omega/2\pi<10^{-3}$ Hz). The palmitate (C_{16}) films are about two decades more conductive than the arachidate (C_{20}) films at both room temperature (291–295 K) and liquid-nitrogen temperature (77 K). The conductance decreases with temperature about a decade for both cases. The data on mixed films, $[C_{16}]_{0.9}$-$[C_{20}]_{0.1}$ and $[C_{16}]_{0.75}$-$[C_{20}]_{0.25}$ at 77 K are taken from the previous work[4] for comparison with those of heterogeneous assemblies.

Figure 3 shows the histrogram of $G(0)$ at 77 K for seven-layer heterogeneous films with six C_{16} and one C_{20} monolayers ($M=6$). The histogram for $[C_{16}]_{0.9}$-$[C_{20}]_{0.1}$ mixed films is also given by the dotted line, since the molar ratio $[C_{16}]:[C_{20}]=9:1$ in the mixture is close to the ratio of layer numbers $M:1=6:1$ in the heterogeneous-assembly films. The patterns of both histograms are, however, fairly different from each other. The distribution for mixed films is single-peaked in the range $\log_{10}G(0)=-10\text{–}-9.5$, while that for the heterogeneous films has two peaks: one is the main peak at $\log_{10}G(0)=-11.5\text{–}-11$, which is even smaller than $\langle\log_{10}G(0)\rangle=-10.22$ for $[C_{16}]_{0.75}$-$[C_{20}]_{0.25}$ films with the molar ratio 3:1, but rather comparable to the single-layer conductance for C_{20}, $\log_{10}7+\langle\log_{10}G(0)\rangle=-11.39$ [Eq. (2)]. The other, the subsidiary peak at $\log_{10}G(0)=-9.5\text{–}-9$, is comparable to the conductance of six C_{16} monolayers, $\log_{10}(\frac{7}{6})+\langle\log_{10}G(0)\rangle=-9.71$.

The heterogeneous-assembly films can be therefore classified into three cases according to the values of $G(0)$ at 77 K:

(I) $\log_{10}G(0)\leq-11$,

(II) $-11<\log_{10}G(0)\leq-10$, and

(III) $\log_{10}G(0)>-10$.

Referring to the values of $G(0)$ in Table I, each case can be interpreted as follows. Case I corresponds to assembly films in which the low-conductance C_{20} monolayers actually govern $G(0)$ in the manner described by Eq. (2), while cases II and III correspond to the imperfect assemblies involving C_{20} layers associated with large-scale imperfections.[1] In case II, the poor quality of the C_{20} layers is reflected in the higher values of $G(0)$, which is still controlled by them. In

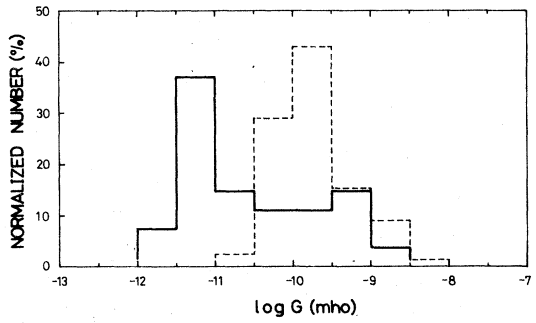

FIG. 3. Normalized histograms of the conductance at 77 K of seven-layer assembly films. The solid and dotted lines refer to heterogeneous films of six C_{16} and one C_{20} monolayers and homogeneous films of $[C_{16}]_{0.9}$-$[C_{20}]_{0.1}$ mixed monolayers, respectively.

TABLE I. Conductance of seven-layer homogeneous assemblies.[a]

Constituent monolayers	Conductance (mho) at room temperature		Conductance in mho at 77 °K	
	$\log_{10}G(0)$	$10^{\langle\log_{10}G(0)\rangle}$	$\log_{10}G(0)$	$10^{\langle\log_{10}G(0)\rangle}$
Cd palmitate (C_{16})	-8.60 ± 0.44	2.5×10^{-9}	-9.78 ± 0.46	1.7×10^{-10}
Cd arachidate (C_{20})	-11.09 ± 0.63	8.1×10^{-12}	-12.24 ± 0.57	5.7×10^{-13}
$[C_{16}]_{0.9}$-$[C_{20}]_{0.1}$	...	...	-9.79 ± 0.46	1.6×10^{-10}
$[C_{16}]_{0.75}$-$[C_{20}]_{0.25}$	...	...	-10.22 ± 0.68	6.1×10^{-11}

[a]Values for mixed assemblies are taken from Ref. 4.

case III, however, the conductance of C_{20} monolayers exceeds that of C_{16} layers, and the $G(0)$'s of the heterogeneous films are determined by the C_{16} monolayers.

The pattern of the histogram in Fig. 3, two peaks separated by a U-shaped valley, for heterogeneous-assembly films, suggests that the single-layer conductance of C_{20} layers is governed by such cooperative mechanisms as to smear out the influence of smaller imperfections, as theoretically predicted in the previous papers.[1,4]

B. Frequency dependence

In the homogeneous-assembly films, the conductance shows very weak frequency dependence within the measurable range of the present experiment. The conductance $G(\omega)$ has approximately the same value as $G(0)$ up to the frequency where $G/\omega C(=\tan\delta)$ goes into the range of 10^{-1} and 10^{-2} at room temperature and 77 K, respectively, and then increases slowly with frequency. This increase is probably due to the component of almost linear variation, $\tan\delta \approx$ const, typically observed in the higher-frequency range 10^{2}–10^{5} Hz.[11] The loss factor of this component is insensitive to the chain length of the constituent acid residue and it is around 10^{-2} and 10^{-3} at room temperature and 77 K, respectively.[12]

Among the three cases I, II, and III of heterogeneous-assembly films, the frequency dispersion of the conductivity was typically observed in case I. Case-III films closely resembled C_{16} homogeneous assemblies in frequency behavior, almost flat for the entire measurable range. Figure 4 shows the $G(\omega)$ and $C(\omega)$ frequency dependence of a heterogeneous-assembly film with $M=6$ and the C_{20} monolayer at the fifth position, Al (base)[$4C_{16}$, $1C_{20}$, , $2C_{16}$]Al. For both room temperature and 77 K, the conductance $G(\omega)$ is constant for the lower frequencies and then jumps upwards by about a decade at certain frequency ranges with a slight decrease in capacitance. An assembly film of $M=8$, Al[$4C_{16}$, $1C_{20}$, $4C_{16}$]Al shows a similar behavior, as seen in Fig. 5.

In the case of assembly films belonging to case I, we found sometimes a very prominent dispersion of $G(\omega)$ associated with an anomalously large $C(\omega)$. Figure 6 shows such an example observed in an Al[$4C_{16}$, $1C_{20}$, $2C_{16}$]Al assembly film. The jump in $G(\omega)$ now covers two decades and the decrease in $C(\omega)$ is correspondingly large, as predicted by the Kramers-Kronig relation [Eq. (4)]. The capacitance at 10^{-1} Hz is, however, still approximately 40% larger than that shown in Fig. 4, regardless of the common structure of both assemblies.

It is suggested that case I is subdivided into two categories; one is the "canonical" case corresponding to assembly films with C_{20} and C_{16} monolayers of high quality, and the other refers to those with anomalous C_{16} monolayers.

It is noted that the films belonging to case II show also a vague but similar frequency dependence to that for case I.

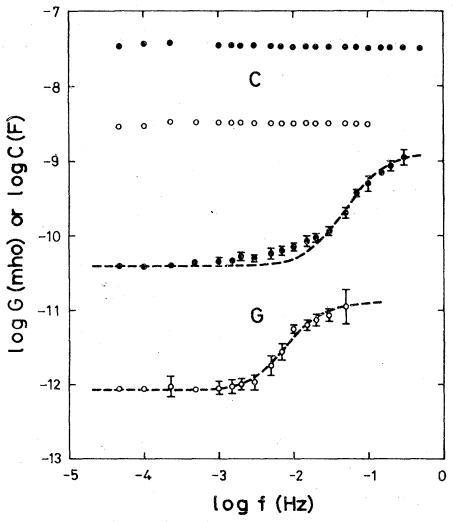

FIG. 4. Frequency-dependence of G and C for an Al[$4C_{16}$, $1C_{20}$, $2C_{16}$]Al junction. The solid and hollow circles refer to room temperature and 77 K, respectively. The data for 77 K are shifted downwards by a decade for clarity.

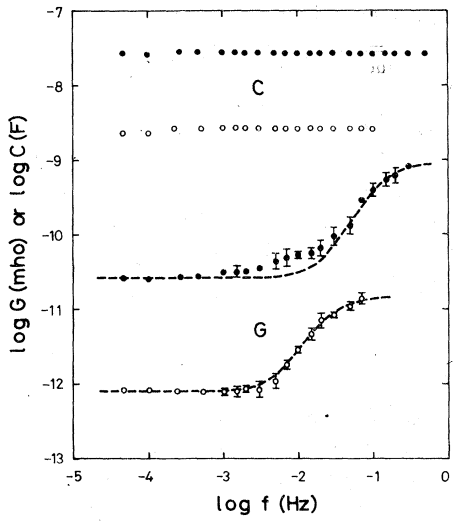

FIG. 5. Frequency dependence of G and C for an Al[$4C_{16}$, $1C_{20}$, $4C_{16}$]Al junction. The solid and hollow circles refer to room temperature and 77 K, respectively. The data for 77 K are shifted downwards by a decade for clarity.

C. Comparison with theoretical predictions

For heterogeneous-assembly films with M C_{16} monolayers and one C_{20} layer, the conductance is given by Eq. (2) as

$$G_M(\omega) = G_M(0) + \frac{G_M(\infty)(f/f_c)^2}{1+(f/f_c)^2} \quad , \tag{6}$$

where $f = \omega/2\pi$ and

$$f_c = \lambda_1/2\pi K(M) \quad . \tag{7}$$

The values of $K(M)$ are analytically given only up to $M=3$. They are $K(1)=\frac{1}{2}$, $K(2)=1$, and $K(3)=1+\frac{1}{2}\sqrt{2}$. For $M \geq 4$, Moore has obtained an empirical relation,

$$K(M) = 0.096(M+1)^2 \quad , \tag{8}$$

from a numerical calculation based on a model of finite one-dimensional arrays of hopping sites.[13] In his model calculation, hopping between remote sites is also taken into account. Let us assume a quadratic form as the expression for the present nearest-neighbor approximation. The coefficients are determined using the above-given values, and the expression is

$$K(M) = 0.103M^2 + 0.189M + 0.207 \quad , \tag{9}$$

which is only slightly different from Eq. (8).

$G_M(0)$ and $G_M(\infty)$ in Eq. (6) are expressed in terms of the seven-layer conductances $G_1(0)$ and $G_2(0)$ for C_{16} and C_{20}, respectively, as

$$G_M(0) = 7G_2(0) \tag{10}$$

and

$$G_M(\infty) = 7MG_1(0)/(M+1)^2 \quad . \tag{11}$$

The capacitance $C_M(\omega)$ is written

$$C_M(\omega) = C_M(\infty) + \Delta C_M/[1+(f/f_c)^2] \quad , \tag{12}$$

using Eq. (4), where

$$\Delta C_M = G_M(\infty)/2\pi f_c \quad , \tag{13}$$

and $C_M(\infty)$ should be approximately equal to the capacitance of $(M+1)$-layer assembly films.

Curves are fitted using Eq. (6) for the data in Figs. 4–6, in which the corresponding characteristics are shown by the dotted lines. The values of the parameters are given in Table II. The capacitance decrease $\Delta C_M = C_m(10^{-3}\ \text{Hz}) - C_M(10^{-1}\ \text{Hz})$ is compared with the calculated value $\Delta C_{M\,\text{calc}}$ obtained by means of Eq. (13).

The values of λ_1 for 77 K are actually comparable to the range 10^{-1} to 10^{-2} Hz given in the previous paper[1] for the corrected thickness, even in the anomalous case [Eq. (6)], although the uncertainty in fitting is considerably large, amounting up to a factor $\pm\log_{10}1.3$.

The seven-layer conductances $G_1(0)$ and $G_2(0)$ for C_{16} and C_{20}, respectively, are calculated employing Eqs. (10) and (11) for each assembly film at each temperature and are listed in Table III. Each value of $G_1(0)$ falls within the standard deviation of the actual seven-layer conductance except for the anomalous case in Fig. 6 with a conductance about a decade larger than the average. This suggests that the rate λ_1 and the carrier concentration n' are rather independent from each other in the actual system. This also favors the l correction in the expression for n' given by Eq. (5). The behaviors of λ_1 and n' will be further

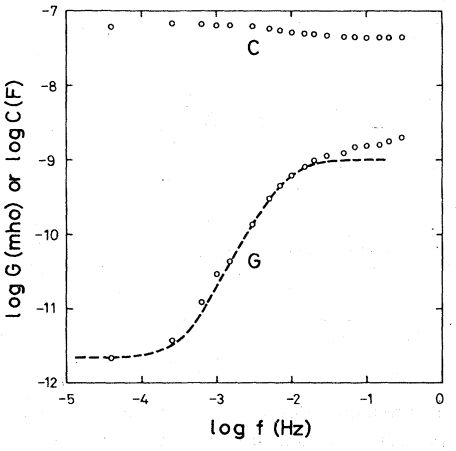

FIG. 6. Example of an anomalously pronounced dispersion observed at 77 K in an Al[$4C_{16}$, $1C_{20}$, $2C_{16}$]Al junction.

TABLE II. Values of parameters obtained by fit.

Reference	Fig. 4	Fig. 5	Fig. 6
M	6	8	6
$G_M(0)$ at RT[a]	4.0×10^{-11}	2.7×10^{-11}	...
(Ω^{-1}) 77 °K	8.5×10^{-12}	8.0×10^{-12}	2.2×10^{-12}
$G_M(\infty)$ at RT	1.2×10^{-9}	9.0×10^{-10}	...
(Ω^{-1}) 77 °K	1.2×10^{-10}	1.4×10^{-10}	1.0×10^{-9}
ΔC_M at RT	2.6×10^{-9}	1.7×10^{-9}	...
(F) 77 °K	1.7×10^{-9}	1.1×10^{-9}	1.9×10^{-8}
$\Delta C_{M\,\mathrm{calc}}$ at RT	1.6×10^{-9}	1.1×10^{-9}	...
(F) 77 °K	1.6×10^{-9}	0.9×10^{-9}	2.0×10^{-8}
f_c at RT	1.2×10^{-1}	1.3×10^{-1}	...
(Hz) 77 °K	1.6×10^{-2}	2.5×10^{-2}	8.0×10^{-3}
λ_1 at RT	3.81	6.79	...
(sec^{-1}) 77 °K	5.08×10^{-1}	1.31	2.54×10^{-1}

[a]RT denotes room temperature.

TABLE III. Parameters calculated from the data in Table II. Values used for the calculation are $2\alpha=1.5\times10^{8}\ \mathrm{cm}^{-1}$, $d=45.3\times10^{-8}$ cm for palmitate ($n=16$) and room temperature (=293 °K).

Reference	Fig. 4	Fig. 5	Fig. 6
$G_1(0)$ at RT[a]	1.40×10^{-9}	1.30×10^{-9}	...
(Ω^{-1}) 77 °K	1.40×10^{-10}	2.0×10^{-10}	1.17×10^{-9}
$G_2(0)$ at RT	5.7×10^{-12}	3.9×10^{-12}	...
(Ω^{-1}) 77 °K	1.21×10^{-12}	1.14×10^{-12}	3.1×10^{-13}
$n'l$ at RT	3.4×10^{9}	2.2×10^{9}	...
(cm^{-2}) 77 °K	6.7×10^{8}	4.7×10^{8}	1.12×10^{10}
N' $(\mathrm{eV}^{-1}\,\mathrm{cm}^{-2})$	4.3×10^{5}	6.4×10^{15}	...
λ_0 (sec^{-1})	1.2×10^{12}	1.4×10^{12}	...
$n'l/kT$ at RT	1.35×10^{11}	8.7×10^{10}	...
$(\mathrm{eV}^{-1}\,\mathrm{cm}^{-2})$ 77 °K	1.01×10^{11}	7.0×10^{10}	1.68×10^{12}

[a]RT denotes room temperature.

discussed in the later paragraphs.

The $G_2(0)$ values are also within the standard deviation of the C_{20} seven-layer conductance given in Table I. The temperature dependence is, however, appreciably weaker than that of the actual seven-layer films. One possible interpretation is that the C_{20} layer in each assembly is still poor in quality and associated with a temperature-insensitive current leak, which predominates towards lower temperatures. The other explanation refers to the limitations inherent in the theory. The dissipation-fluctuation theorem,[14] on which the extended Montroll-Weiss formalism[6] is based, is, as is well known, a linear-response theory treating the external field as a small perturbation, which exerts its influence upon the thermally fluctuating carrier concentration. The field induced in turn by the charge is therefore neglected in the theory. In the actual system, however, the C_{20} monolayer will be polarized by the charge accumulated at both interfaces, and the carrier transport may be enhanced by the increased field for $f \ll f_c$. This mechanism will work more dominantly for lower temperatures and for larger unit cells. It should be noted that we have not yet obtained a sufficient number of the "canonical case" dispersion characteristics to present the average and standard deviation for each parameter, based on a reasonable analysis of the histogram pattern, although the measurement carried out so far indicates each standard deviation to be appreciably smaller than a decade.

Let us proceed to examine whether the Maxwell-Wagner effect is involved or not. The scheme discussed above can be represented by an equivalent circuit as shown in Fig. 7(a), while the equivalent circuit for the Maxwell-Wagner effect is given by (b). The characteristic frequency is in this case given as[15]

$$f_c' = [G_1(0) + MG_2(0)]/2\pi(C_1 + MC_2) \ , \qquad (14)$$

where C_1 and C_2 are the capacitances of seven-layer assembly films of C_{16} and C_{20}, respectively. They are $C_1^{-1} = (3.3 \pm 0.3)\times10^{7}\ \mathrm{F}^{-1}$ and $C_2^{-1} = (4.6 \pm 0.3)\times10^{7}\ \mathrm{F}^{-1}$ at 77 K. Taking the values $C_1 = 3\times10^{-8}$ F and $C_2 = 2\times10^{-8}$ F together with $G_1(0) = 2\times10^{-10}$ mho and $G_2(0) = 6\times10^{-13}$ mho, we obtain the characteristic frequencies

$$f_c' = 2.2\times10^{-4}\ \mathrm{Hz} \quad \text{for } M = 6 \qquad (15)$$

and

$$f_c' = 1.7\times10^{-4}\ \mathrm{Hz} \quad \text{for } M = 8 \ , \qquad (16)$$

which are by about two decades smaller than the corresponding f_c in Table II. The Maxwell-Wagner effect is therefore eliminated as a possible mechanism. It is suggested that a structure-dependent dispersion of this type is observable only for smaller unit-cell size, since, as M increases, $f_c \propto M^{-2}$ [Eqs. (7) and (9)] and $f_c' \propto M^{-1}$ [Eq. (14)] for the microscopic and macroscopic processes, respectively, for the realistic case $G_1/G_2 \gg M$. Therefore from a certain M on, the Maxwell-Wagner effect will predominate as the relaxation mechanism.

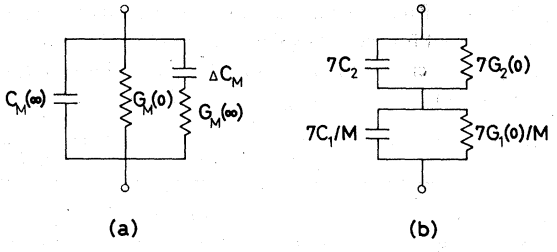

FIG. 7. Equivalent circuits for the actually observed dispersion (a) and the Maxwell-Wagner effect (b).

Let us evaluate the values of $n'l$, N', and λ_0, which are, in the present theoretical framework, common to Cd salts of different fatty acids. The values listed in Table III are calculated from the data in Table II by assuming $2\alpha = 1.5 \times 10^8$ cm^{-1} as in the previous works[3,4] and the corrected value of the thickness, $l = nd/(2n+5) = 45.3 \times \frac{16}{37} = 19.6 \times 10^{-8}$ cm,[7] by means of the equations

$$n'l = (kT/e^2)(M+1)^2 G_M(\infty)/MA\lambda(T) \quad , \tag{17}$$

$$N' = \left(\frac{4\alpha}{\pi lk}\right) \frac{(\sqrt{T_1}-\sqrt{T_2})^2}{T_1 T_2 [\ln[\lambda(T_1)/\lambda(T_2)]]^2} \quad , \tag{18}$$

and,

$$\lambda_0 = (2\alpha l)^{-3/2} e^{2\alpha l} \times \exp\left(\frac{\ln[\lambda(T_1)^{\sqrt{T_1}}/\lambda(T_2)^{\sqrt{T_2}}]}{\sqrt{T_1}-\sqrt{T_2}}\right) \quad , \tag{19}$$

where $A = 0.2$ cm^2 is the electrode area, and T_1 and T_2 are 293 K and 77 K, respectively. In deriving Eq. (17), we have ignored the difference between $\frac{1}{2}d$ and l.

N' and λ_0 are of the order of 10^{15} eV^{-1} cm^{-2} and 10^{12} sec^{-1}, respectively, coinciding with those estimated in the earlier works.[2-5]

The values of $n'l/kT$ are also listed in Table III for comparison with N'. The difference in magnitude is more than four decades, indicating the inadequacy of Eq. (5) to give the effective carrier concentration. However, $n'l/kT$ is almost constant for both temperatures, in each case within fitting error. $n'l/kT \approx$ const. or $n'l \propto T$ agrees qualitatively with Eq. (5) and thus with the actually observed $T^{-1/2}$ conductivity.[4] It is now clarified that the effective carrier concentration should be explained by models other than the degenerate electron system with a smooth $N'(E)$ at each interface adopted in the earlier works.[3-5] We note that the temperature dependence of $n'l$ can be simulated by assuming appropriate donor and acceptor levels.

IV. CONCLUSION

In Sec. III, we have seen that the introduction of one single Cd-arachidate monolayer into a Cd-palmitate layer system causes a drastic reduction of dc conductance, quite in contrast to the case of mixing of both constituents.[4] This confirms the validity of the scheme adopted so far, with a single rate and nearest-neighbor approximation, as the appropriate model to describe the actual multilayer-assembly system.

Conductivity dispersion has been actually observed in heterogeneous-assembly films of Cd-palmitate and Cd-arachidate monolayers, where the Maxwell-Wagner effect has been duly eliminated from the possible mechanisms. The hopping transition rate in Cd-palmitate has been evaluated from the characteristic dispersion frequency to be of the order of 1 sec^{-1} at room temperature and around 10^{-1}–1 sec^{-1} at 77 K, which values agree with those calculated employing the corrected monolayer thickness allowing for finite interface thickness.

The values of the common parameters, the interface state density N' and λ_0, agree in order of magnitude with those estimated before, 10^{15} eV^{-1} cm^{-2} and 10^{12} sec^{-1}. The effective carrier concentration n' is found to be rather independent of N'. This indicates the inadequacy of the estimate based on the two-dimensional degenerate electron system with slowly varying $N'(E)$ adopted in the earlier works.[3-5] It is nevertheless indicated that n' is roughly proportional to the temperature and thus the temperature dependence of conductivity is mainly due to that of the transition rate, which is the case in the earlier scheme.

ACKNOWLEDGMENTS

The authors wish to thank Dr. H. Okushi and Dr. K. Tanaka for their valuable comments.

[1] M. Sugi and S. Iizima, Phys. Rev. B 15, 574 (1977).
[2] M. Sugi, K. Nembach, D. Möbius, and H. Kuhn, Solid State Commun. 15, 1867 (1974).
[3] M. Sugi, T. Fukui, and S. Iizima, Appl. Phys. Lett. 27, 559 (1975); 28, 240 (1976).
[4] S. Iizima and M. Sugi, Appl. Phys. Lett. 28, 548 (1976).
[5] M. Sugi, T. Fukui, and S. Iizima, Chem. Phys. Lett. 45, 163 (1977).
[6] H. Scher and M. Lax, Phys. Rev. B 7, 4502 (1973).
[7] A. Matsuda, M. Sugi, T. Fukui, S. Iizima, M. Miyahara, and

Y. Otsubo, J. Appl. Phys. 48, 771 (1977).
[8]H. Kuhn, D. Möbius, and H. Bücher, in *Techniques of Chemistry*, edited by A. Weissberger and B. W. Rossiter (Wiley, New York, 1973), Vol. 1, Part IIIB.
[9]K. B. Blodgett, J. Am. Chem. Soc. 57, 1007 (1935).
[10]T. Fukui, A. Matsuda, M. Sugi, and S. Iizima, Bull. Electrotech. Lab. 41, 423 (1977).
[11]M. Sugi, K. Nembach, D. Möbius, and H. Kuhn, Solid State Commun. 13, 603 (1973).
[12]S. Iizima (unpublished).
[13]E. J. Moore, J. Phys. C 7, 1840 (1974).
[14]R. Kubo, J. Phys. Soc. Jpn. 12, 570 (1957).
[15]W. F. Brown, Jr., in *Handbuch der Physik*, edited by S. Flügge (Springer, Berlin, 1956), Vol. XVII.